

# The effects of interactions and disorder in the two-dimensional chiral metal

J. J. Betouras and J. T. Chalker

*Theoretical Physics, Oxford University, 1 Keble Road, Oxford, OX1 3NP, United Kingdom*  
(November 4, 2018)

We study the two-dimensional chiral metal, which is formed at the surface of a layered three-dimensional system exhibiting the integer quantum Hall effect by hybridization of the edge states associated with each layer of the sample. We investigate mesoscopic fluctuations, dynamical screening and inelastic scattering in the chiral metal, focussing particularly on fluctuations of conductance,  $\delta g(B)$ , with magnetic field,  $B$ . The correlation function  $\langle \delta g(B) \delta g(B + \delta B) \rangle$  provides information on the inelastic scattering rate,  $\tau_{in}^{-1}$ , through both the variance of fluctuations and the range of correlations in  $\delta B$ . We calculate this correlation function for samples which are not fully phase coherent. Two regimes of behaviour exist, according to whether  $\tau_{in}^{-1}$  is smaller or larger than  $\tau_{\perp}^{-1}$ , the rate for inter-edge tunneling, and we give results in both regimes. We also investigate dynamical screening of Coulomb interactions in the chiral metal and calculate the contribution to  $\tau_{in}^{-1}$  from electron-electron scattering, finding  $\tau_{in}^{-1} \propto T^{3/2}$  for  $\tau_{in}^{-1} \ll \tau_{\perp}^{-1}$  at temperature  $T$ .

PACS numbers: 73.40.Hm, 73.23.-b, 73.20.-r, 72.15.Lh

## I. INTRODUCTION

An unusual type of two-dimensional conductor, the chiral metal, may be formed at the surface of a layered, three-dimensional system in the presence of a magnetic field which has a component perpendicular to the layers<sup>1–3</sup>. It occurs in a system of weakly-coupled layers at magnetic field-strengths for which an isolated layer would have an integer quantised Hall conductance. Under these circumstances, bulk states are localised and the extended, chiral edge states associated with each layer hybridise to form a two-dimensional conductor at the surface of the sample. Properties of this chiral metal may be probed by conductance measurements with current flow normal to the layers.

Early experimental work on semiconductor multilayer samples<sup>4</sup> established that the integer quantum Hall effect of a single layer is indeed robust against weak interlayer tunneling, and suggested that, within a quantum Hall plateau, interlayer conductivity in the bulk vanishes in the low-temperature limit. Subsequent theoretical discussions<sup>1,2</sup> drew attention to the unusual nature of surface states in multilayer quantum Hall systems, and some aspects of the theory of the chiral metal have since been explored in considerable detail<sup>5–16</sup>. Recent experiments by Druist *et al* have isolated the contribution of surface states to vertical transport<sup>3</sup> and demonstrated that mesoscopic conductance fluctuations offer a way to study inelastic scattering in the chiral metal<sup>17,18</sup>. Conduction by surface states has also been invoked in the interpretation of further experiments on semiconductor multilayer samples<sup>19</sup>, and on the bulk quantum Hall effect in both organic conductors<sup>20</sup> and an inorganic quasi-two dimensional conductor<sup>21</sup>.

In this paper we extend the theoretical treatment of mesoscopic chiral conductors in two respects. First, we develop some aspects of the theory of conductance fluctuations which we hope will be useful for the interpretation

of experiments. Second, we study electron-electron interactions in the dirty chiral metal.

The existing understanding of conductance fluctuations in the chiral metal is based on calculations<sup>6,7,10</sup> for the variance of sample-to-sample conductance fluctuations in systems that are fully phase-coherent. From the results of those calculations, estimates have been made<sup>11</sup> for the variance of conductance fluctuations measured as a function of magnetic field in samples that are only partially phase-coherent, and also for the range in magnetic field of conductance correlations. These estimates determine the relevant scales but do not yield numerical coefficients or functional forms. Moreover, they depend on a continuum treatment of the system of coupled edge states, and apply if the inelastic scattering rate,  $\tau_{in}^{-1}$ , is smaller than the inter-edge tunneling rate,  $\tau_{\perp}^{-1}$ , while existing experiments appear to be in the opposite regime<sup>17,18</sup>. We supplement this past work by calculating in full the conductance correlation function  $\langle \delta g(B) \delta g(B + \delta B) \rangle$ , both for  $\tau_{in}^{-1} \ll \tau_{\perp}^{-1}$  and for  $\tau_{in}^{-1} \gg \tau_{\perp}^{-1}$ .

Separately, we consider conductance as a function of Fermi energy. For conventional disordered conductors, changes in Fermi energy provide a way to sample the conductance distribution. In contrast, we find that the conductance of a partially-coherent chiral metal sample, though dependent on the disorder realisation, is unchanged by small variations in Fermi energy. One consequence is that thermal smearing of the electron distribution function does not decrease the amplitude of conductance fluctuations in the chiral metal.

Turning to electron-electron interactions, we establish the form of the dynamically screened interaction and examine some of its consequences. Most importantly, we calculate the inelastic scattering rate due to electron-electron interactions, obtaining  $\tau_{in}^{-1} \propto T^{3/2}$  for  $\tau_{in} \gg \tau_{\perp}$ . We also examine other interaction effects which are known to be of interest in conventional disor-

dered conductors<sup>22</sup>. Interactions in diffusive metals are responsible for a zero-bias anomaly in the tunneling density of states<sup>23</sup>, but – as noted previously<sup>2</sup>, and as we confirm – this is absent from the chiral metal. Similarly, the leading interaction contribution to the mean conductance has a singular temperature dependence in conventional disordered conductors<sup>24–26</sup>, but we find that it cancels in the chiral metal.

The remaining sections of this paper are organised as follows. We review briefly past work and collect our most important new results in Sec. II. We describe calculations on conductance fluctuations in Sec. III, and treat electron-electron interactions in Sec. IV. We summarise and discuss recent experiments in Sec. V.

## II. BACKGROUND AND MAIN RESULTS

It is useful first to introduce some notation. Consider a layered sample which exhibits the bulk quantum Hall effect, with one Landau level below the Fermi energy. A chiral metal is formed at the sample surface, from hybridisation of one edge state per layer. We denote the interlayer spacing by  $a$ , the chiral velocity by  $v$  and the interlayer diffusion constant by  $D$ . The electron density of states per unit area is  $n = 1/hva$  and the surface conductivity in the transverse direction, as given by the Einstein relation, is  $\sigma = D/va$ , in units of  $e^2/h$ , which we use throughout this paper.

Phase coherent mesoscopic conductors are known to have three distinct mesoscopic regimes, according to relative sample dimensions<sup>10</sup>. For definiteness, suppose that the sample is a cylinder of height  $L$  and circumference  $C$ , with its axis perpendicular to the layers. Take the number of layers to be  $N$ , so that  $L = Na$ . Two intrinsic length scales arise, with which  $L$  should be compared. The first of these involves the mean conductance of the sample, which if Ohm's law applies is  $\langle g \rangle = C\sigma/L$ : the quasi one-dimensional localisation length,  $\xi = 2C\sigma$ , is the value of  $L$  at which  $\langle g \rangle$  is of order the quantum unit of conductance. Samples with  $L \gg \xi$  have states localised in the vertical direction and are quasi one-dimensional insulators. Samples with  $L \ll \xi$  are metallic and have Ohmic dependence of  $\langle g \rangle$  on sample dimensions. A second length scale influences the amplitude of conductance fluctuations. It is the distance  $L_1$  that an electron diffuses in the transverse direction during the time taken to circumnavigate the sample:  $L_1 = (DC/v)^{1/2} \equiv (a\sigma C)^{1/2}$ . Samples with  $L_1 \ll L \ll \xi$  are quasi one-dimensional metals without time-reversal symmetry and, in common with other examples of such systems, have a variance for the conductance of  $\langle (\delta g)^2 \rangle = 1/15$ . Samples with  $L \ll L_1$  are two-dimensional chiral metals. If contacts are attached to these samples for conductance measurements, electrons will escape by diffusion to the contacts before completing a circuit of the sample in the chiral direction. As a result, multiple scattering of an

electron from a given impurity is completely suppressed. Such samples present a number of essentially independent parallel strips for conduction in the transverse direction, each having a width in the chiral direction given by the distance an electron propagates before reaching a contact. This width is  $L^2v/D \equiv C(L/L_1)^2$ . The conductance of the two-dimensional chiral metal may be thought of<sup>6</sup> as a sum of contributions from each such strip, and its variance has the value<sup>6,10</sup>  $\langle \delta g^2 \rangle = L_1^2/3L^2$ .

Our concern in the following is with samples that are not completely phase coherent. They have two different metallic regimes, analogous to those described above for phase coherent conductors. We restrict our attention to one of these, the incoherent two-dimensional metal, in which  $\tau_{in} < C/v$  so that dephasing occurs before circumnavigation: this is the simpler regime theoretically and seems the one relevant for existing experiments. Cho, Balents and Fisher<sup>11</sup> have estimated the size of conductance fluctuations in the incoherent metal by viewing each phase-coherent region as a classical resistor and the whole sample as a random resistor network. We summarise their argument here for convenience. Let the number of regions into which the sample is divided be  $n_x$  in the chiral direction, and  $n_z$  in the transverse direction. Let the conductance of a single region have mean value  $g_{\text{patch}}$ , with fluctuations of magnitude  $\delta g_{\text{patch}}$ ; provided  $\delta g_{\text{patch}} \ll g_{\text{patch}}$ , the corresponding resistances are  $R_{\text{patch}} = 1/g_{\text{patch}}$  and  $\delta R_{\text{patch}} = \delta g_{\text{patch}}/g_{\text{patch}}^2$ . A strip of  $n_z$  such regions forms a single conduction path in the transverse direction, having mean resistance  $R_{\text{strip}} = n_z R_{\text{patch}}$  with fluctuations  $\delta R_{\text{strip}}^2 = n_z \delta R_{\text{patch}}^2$ ; the corresponding conductances are  $g_{\text{strip}} = 1/R_{\text{strip}}$  and  $\delta g_{\text{strip}} = \delta R_{\text{strip}}/R_{\text{strip}}^2$ . Since the sample consists of  $n_x$  such paths in parallel, its conductance has mean value  $\langle g \rangle = n_x g_{\text{strip}} = (n_x/n_z)g_{\text{patch}}$  and fluctuations  $\langle \delta g^2 \rangle = n_x \delta g_{\text{strip}}^2 = (n_x/n_z^3)\delta g_{\text{patch}}^2$ . The implications of this final result depend on the size of a patch in the transverse direction, compared to the layer spacing,  $a$ .

If  $\tau_{in}^{-1} \ll \tau_{\perp}^{-1}$  so that the phase coherence length in the transverse direction is much larger than the layer spacing, which is the case considered previously<sup>11</sup>, then one expects a continuum treatment of the system to be adequate. In this case,  $n_z^2 = L^2/D\tau_{in}$  and  $\delta g_{\text{patch}}^2 \sim 1$ ; in addition,  $n_x = C/v\tau_{in}$ . Combining these expressions and introducing the inelastic scattering length in the chiral direction,  $l_{in} = v\tau_{in}$ , one arrives at the conclusion (Eq. (4.1) of Ref. 11) that

$$\langle \delta g^2 \rangle \sim \left( \frac{l_{in}}{C} \right)^{1/2} \cdot \left( \frac{\langle g \rangle}{N} \right)^{3/2}. \quad (2.1)$$

Experimental studies use a magnetic field with a component normal to the sample surface to generate conductance fluctuations in the chiral metal<sup>3,17</sup>; the field scale of conductance correlations is set by the flux quantum,  $\Phi_0$ , and the area of a coherent region, being (Eq. (4.4) of

Ref. 11)

$$\delta B_0 \sim \Phi_0 / (l_{in}^{3/2} a^{1/2} \sigma). \quad (2.2)$$

The results we obtain in Sec. III substitute for Eqns. (2.1) and (2.2) the correlation function

$$\langle \delta g(B_\perp) \delta g(B_\perp + \delta B) \rangle = \left( \frac{\langle g \rangle}{N} \right)^{3/2} \cdot \left( \frac{l_{in}}{C} \right)^{1/2} \cdot f(y) \quad (2.3)$$

where the function  $f(y)$  is

$$f(y) = \pi^{-1/2} \int_{-\infty}^{\infty} dx e^{-(x^2 + yx^6)} \quad (2.4)$$

with the scaling variable

$$y = \frac{\pi^2}{12} \cdot \sigma \cdot a l_{in}^3 \cdot \left( \frac{\delta B}{\Phi_0} \right)^2. \quad (2.5)$$

The opposite limit of weakly coupled edges,  $\tau_{in}^{-1} \gg \tau_\perp^{-1}$ , has not previously been examined theoretically but seems to be important experimentally<sup>17,18</sup>. Adapting the argument outlined above, we take, as elements of a classical resistor network, regions again of length  $l_{in}$  in the chiral direction but now of width  $a$  in the transverse direction. Then  $n_x = C/l_{in}$  and  $n_z = N$ . The mean conductance of one such patch is small in this limit. We expect fluctuations to be of the same order, and take  $\delta g_{\text{patch}}^2 \sim g_{\text{patch}}^2 = (\langle g \rangle n_z / n_x)^2$ . In this way we obtain in place of Eq. (2.1)

$$\langle \delta g^2 \rangle \sim \frac{\langle g \rangle^2}{N} \cdot \frac{l_{in}}{C}. \quad (2.6)$$

The field scale of conductance correlations is again set by the flux quantum and the area of a coherent region, but Eq. 2.2 is replaced in this limit by

$$\delta B_0 \sim \Phi_0 / (l_{in} a). \quad (2.7)$$

We calculate in Sec. III the conductance correlation function for weakly coupled edges, finding in agreement with these estimates

$$\langle \delta g(B_\perp) \delta g(B_\perp + \delta B) \rangle = \frac{2\langle g \rangle^2}{NC} \frac{l_{in}}{1 + z^2} \quad (2.8)$$

where  $z = 2\pi\delta Bl_{in}a/\Phi_0$ .

The inelastic scattering length,  $l_{in}$ , appears as a phenomenological parameter in the expressions given above for the correlation function of conductance fluctuations. The contribution to inelastic scattering from electron-electron interactions is known in non-chiral dirty metals to have a characteristic temperature dependence, reflecting the form of the dynamically screened Coulomb interaction in a diffusive system<sup>22,27-29</sup>, and it is interesting

to study inelastic scattering microscopically for the chiral metal. We do this in Sec. IV, examining dynamical screening and using the results to calculate the inelastic scattering rate,  $\tau_{in}^{-1}$ . We obtain in the regime  $\tau_{in}^{-1} \ll \tau_\perp^{-1}$

$$\tau_{in}^{-1} = c \frac{a}{D^{1/2}} \left( \frac{k_B T}{\hbar} \right)^{3/2}, \quad (2.9)$$

where  $c \approx 1.5$  is a dimensionless coefficient. A simple interpretation of this result can be given, following similar arguments established in the theory of diffusive metals<sup>22</sup>. As a starting point, note that (in both chiral and non-chiral diffusive metals) the dynamically screened interaction strength at long wavelengths is independent of the bare interaction strength. In consequence, the inelastic scattering rate depends only on properties of the non-interacting system and temperature:  $\hbar\tau_{in}^{-1}$  is of order the single-particle energy level spacing in a system with dimensions determined by the distance an electron moves in the time  $\hbar/k_B T$ . These dimensions are  $L_x(T) \sim \hbar v / k_B T$  and  $L_z(T) \sim (\hbar D / k_B T)^{1/2}$  in the chiral and transverse directions respectively, and the estimate  $\tau_{in}^{-1} \sim (\hbar n L_x(T) L_z(T))^{-1}$  is consistent with Eq. (2.9). An equivalent argument applied to non-chiral, diffusive conductors in  $d$ -dimensions yields  $\tau_{in}^{-1} \sim T^{d/2}$ , which is corrected in two dimensions to  $\tau_{in}^{-1} \sim T |\log(T)|$  by detailed calculations<sup>22,29</sup>. The factor of  $\log(T)$  in this last expression reflects divergent contributions to scattering in the diffusive two-dimensional metal, from processes with small energy transfer. The same scattering processes are responsible for a difference, in diffusive two-dimensional metals, between the temperature dependence of the inelastic (or out-scattering) rate, which acts as a cut-off for conductance fluctuations, and the dephasing rate, which acts as a cut-off for the weak localisation effects that result in negative magnetoresistance. In the chiral metal, as for conventional, diffusive metals in more than two dimensions, small energy transfer processes are not dominant and there is a single relaxation rate.

Inelastic scattering in weakly coupled edge states has been discussed in Ref. 2, where it is noted that one expects  $\tau_{in}^{-1} \propto T$  from perturbation theory in the interaction strength, applied to a single edge.

### III. CONDUCTANCE FLUCTUATIONS

#### A. Model

We study conductance fluctuations in the chiral metal using a single-particle description of the system, supplemented by a relaxation rate to represent inelastic scattering. We treat a sample with layers lying in the  $x - y$  plane and consider a surface in the  $x - z$  plane. Electrons on the surface then have a continuous coordinate,  $x$ , in the chiral direction parallel to the edges of layers, and an integer coordinate,  $n$ , labeling layers in the transverse ( $z$ ) direction, which we combine as  $\mathbf{r} = (x, n)$ . We take

the interlayer tunneling energy to be  $t$  and represent a magnetic field component,  $B_\perp$ , normal to the surface using the vector potential  $\mathbf{A} = B_\perp a \mathbf{\hat{x}}$ . The Hamiltonian  $H$  acts on a wavefunction  $\psi_n(x)$  according to<sup>2,15</sup>

$$(H\psi)_n(x) = v(-i\hbar\partial_x + eB_\perp an)\psi_n(x) - t[\psi_{n+1}(x) + \psi_{n-1}(x)] + V_n(x)\psi_n(x), \quad (3.1)$$

$$(3.2)$$

where  $V_n(x)$  is a random potential arising from impurities and surface roughness. We choose  $V_n(x)$  to be Gaussian distributed with short-range correlations, so that  $\langle V_n(x) \rangle = 0$  and  $\langle V_n(x) V_m(x') \rangle = \Delta \delta_{nm} \delta(x - x')$ .

Denoting the Green's function for Eq. (3.1) by  $g \equiv (z - H)^{-1}$ , we require its disorder average

$$G(z; \mathbf{r}_1, \mathbf{r}_2) \equiv \langle g(z; \mathbf{r}_1, \mathbf{r}_2) \rangle, \quad (3.3)$$

the diffusion propagator

$$K(\omega; \mathbf{r}_1, \mathbf{r}_2) \equiv \langle g(\omega + i0; \mathbf{r}_1, \mathbf{r}_2) g(-i0; \mathbf{r}_2, \mathbf{r}_1) \rangle, \quad (3.4)$$

and its Fourier transform

$$K(\omega, \mathbf{k}) \equiv \int_{-\infty}^{\infty} dx \sum_n e^{i(xk_x + ank_y)} K(\omega; \mathbf{0}, \mathbf{r}). \quad (3.5)$$

These quantities are known from calculations<sup>2,15</sup> using the usual expansion in powers of the Green's function for the disorder-free system. Without disorder or a normal magnetic field component, eigenstates are plane waves and the electron dispersion relation is  $\epsilon(\mathbf{k}) = \hbar v k_x - 2t \cos(k_z a)$ . This dispersion along with the chiral motion leads to an open Fermi surface on which all electrons have the same  $x$ -component of velocity. In the presence of a normal magnetic field component of dimensionless strength  $b \equiv eB_\perp va/t$ , the eigenfunctions  $\psi_n(x)$  in the pure system are

$$\psi_n(x) = \frac{1}{\sqrt{2\pi}} e^{ikx} \phi_\alpha(n), \quad (3.6)$$

where  $\alpha$  is an integer and  $\phi_\alpha(n) = J_{n-\alpha}(2/b)$ , the Bessel function of order  $n - \alpha$ . The associated energy eigenvalues are  $\hbar v k + \epsilon_\alpha$  with  $\epsilon_\alpha = abt$ .

The treatment of disorder is simple in some respects because chiral motion prevents multiple scattering of an electron from any particular impurity. As a result, the average one-particle Green's function is given exactly by the Born approximation<sup>2,15</sup>. In this way, one arrives at<sup>15</sup>

$$G^R(E; \mathbf{r}_1, \mathbf{r}_2) = \frac{1}{2\pi} \int_{-\infty}^{\infty} dk \sum_\alpha \frac{e^{ik(x_2 - x_1)} \phi_\alpha(n_1) \phi_\alpha(n_2)}{E + i\Delta/(2\hbar v) - (\hbar v k + \epsilon_\alpha)}, \quad (3.7)$$

where we use the standard notation,  $G^R(E) \equiv G(E + i0)$  and  $G^A(E) \equiv G(E - i0)$ . From the value of the self-energy, the elastic scattering time is  $\tau_{el} = \hbar^2 v / \Delta$ , and the

elastic scattering length is  $l_{el} = (\hbar v)^2 / \Delta$ . In the absence of a normal magnetic field component,  $G^R(E; \mathbf{r}_1, \mathbf{r}_2)$  is translationally invariant and has the Fourier transform

$$G^R(E; \mathbf{k}) = [E + i\Delta/(2\hbar v) - (\hbar v k_x - 2t \cos(k_z a))]^{-1}. \quad (3.8)$$

For non-zero  $B_\perp$ ,  $G^R(E; \mathbf{r}_1, \mathbf{r}_2)$  acquires a phase under translations, which is central to calculations of conductance fluctuations with magnetic field:

$$G^R(E; \mathbf{0}, \mathbf{r}) = \exp(i\beta an' x) G^R(E; \mathbf{r}', \mathbf{r} + \mathbf{r}'), \quad (3.9)$$

where  $\beta = 2\pi B_\perp / \Phi_0$ ,  $\mathbf{r} = (x, n)$  and  $\mathbf{r}' = (x', n')$ .

The diffusion propagator is similarly given by a sum of ladder diagrams, and has a form that reflects the combination of chiral motion in  $x$  and diffusion in  $z$ . At small wavevectors it is

$$K(\omega, \mathbf{k}) = (\hbar v)^{-1} [\hbar D k_z^2 - i(\omega + \hbar v k_x)]^{-1}. \quad (3.10)$$

The diffusion constant has the value  $D = 2(at)^2 v / \Delta$  in the absence of a normal magnetic field component, and has the field dependence<sup>15</sup>  $D(B_\perp) = D(0) / [1 + (B_\perp / B_0)^2]$ , where the field scale for magnetoresistance is  $B_0 = \Phi_0 / al_{el}$ .

Because of the simplifications in the treatment of disorder that follow from chiral motion, the results above hold both at weak disorder ( $t \gg \Delta / (\hbar v)$ ) and at strong disorder ( $t \ll \Delta / (\hbar v)$ ). In a semiclassical description, electron motion follows a random walk in the transverse direction. At weak disorder, steps of the walk have speed  $at/\hbar$  and duration  $\tau_{el}$ ; the rate for inter-edge tunneling is  $\tau_\perp^{-1} = t/\hbar$ . At strong disorder, steps are of length  $a$  and duration  $\tau_\perp$ ; from the value of  $D$ , we deduce that the rate for inter-edge tunneling is then  $\tau_\perp^{-1} = (t/\hbar)^2 \tau_{el}$ .

## B. Conductivity

The component of the current density operator in the transverse direction is

$$j_z(\mathbf{r}) = \frac{e a t}{i \hbar} [\psi_n^*(x) \psi_{n+1}(x) - \psi_{n+1}^*(x) \psi_n(x)]. \quad (3.11)$$

The Kubo formula for the transverse conductivity in a system of area  $A$  is

$$\sigma = \frac{\hbar}{2\pi A} \text{Tr}[j_z g^R j_z g^A]. \quad (3.12)$$

Evaluating the disorder average of this expression, one finds

$$\sigma = \frac{e^2}{h} \frac{D}{va} \quad (3.13)$$

as expected from the Einstein relation.

### C. Conductance fluctuations in magnetic field

Conductance fluctuations have been studied previously<sup>6,7,10</sup> for the two-dimensional chiral metal in the absence of inelastic scattering, in most detail by Gruzberg, Read and Sachdev<sup>10</sup>, who discussed the variance and its dependence on sample geometry. Here we present calculations which include inelastic scattering, obtaining the correlation function

$$F(\delta B) = \langle \delta g(B) \delta g(B + \delta B) \rangle. \quad (3.14)$$

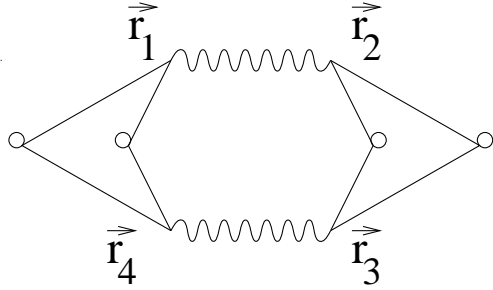


FIG. 1. The Feynman diagram which is relevant for the conductance fluctuations: current operators are represented by circles, one-particle Green's functions by straight lines, and diffusion propagators by wavy lines.

As a result of chiral motion, and provided that electrons do not circumnavigate the sample phase coherently ( $C/v > \tau_{in}$  or  $C/v > L^2/D$ ), the only one-loop diagram contributing to  $F(\delta B)$  is the one shown in Fig. 1. It is most conveniently evaluated in real space, and represents the expression

$$F(\delta B) = \int \sum_{n_i} K_{\delta B}(\mathbf{r}_1, \mathbf{r}_2) K_{\delta B}^*(\mathbf{r}_4, \mathbf{r}_3) J(\mathbf{r}_1, \mathbf{r}_4) J(\mathbf{r}_2, \mathbf{r}_3) d\{x_i\}. \quad (3.15)$$

Here,  $K_{\delta B}(\mathbf{r}_1, \mathbf{r}_2)$  stands for the zero-frequency diffusion propagator, generalised to the situation of interest, in which the two Green's functions entering it are evaluated for different normal magnetic field strengths,

$$K_{\delta B}(\mathbf{r}, \mathbf{r}') = \langle g_B^R(\mathbf{r}, \mathbf{r}') g_{B+\delta B}^A(\mathbf{r}', \mathbf{r}) \rangle, \quad (3.16)$$

and in which inelastic scattering is included. The other factors arise from a combination of single-particle Green's functions and current operators, and are short range:  $J(\mathbf{r}, \mathbf{r}') = (\hbar \Delta^2 / 2\pi L^2) |C(\mathbf{r}, \mathbf{r}')|^2$ , with

$$C(\mathbf{r}, \mathbf{r}') = \int \sum_{n_1} G^A(\mathbf{r}, \mathbf{r}_1) j_z(\mathbf{r}_1) G^R(\mathbf{r}_1, \mathbf{r}') dx_1. \quad (3.17)$$

Our approach to evaluating  $F(\delta B)$  is different in the two regimes,  $\tau_{in}^{-1} \ll \tau_{\perp}$  and  $\tau_{in}^{-1} \gg \tau_{\perp}$ , which we consider separately.

#### 1. Strongly coupled edges: $\tau_{\perp}^{-1} \gg \tau_{in}^{-1}$

In this regime, the discreteness of the system in the transverse direction may be neglected. It is sufficient to approximate the short-range terms in Eq. (3.15) by

$$J(\mathbf{r}, \mathbf{r}') = J_0 \delta(\mathbf{r} - \mathbf{r}'), \quad (3.18)$$

where

$$J_0 = \frac{e^2}{h} \frac{4(at)^2}{\Delta L^2} (\hbar v)^2. \quad (3.19)$$

The diffusion propagator, generalised to include the magnetic field difference  $\delta B$  and inelastic scattering, is most easily calculated within a continuum treatment of the transverse direction by solving, for  $x > 0$ , the differential equation

$$v \partial_x K_{\delta B}(\mathbf{0}, \mathbf{r}) = [D \partial_z^2 + iv\delta\beta z - \tau_{in}^{-1}] K_{\delta B}(\mathbf{0}, \mathbf{r}) \quad (3.20)$$

with the initial condition  $K_{\delta B}(\mathbf{0}; x, z) = (\hbar v)^{-2} \delta(z)$  at  $x = 0$ . Here, the inelastic scattering rate,  $\tau_{in}^{-1}$ , has been introduced,

and the magnetic field difference enters through  $\delta\beta \equiv (2\pi\delta B/\Phi_0)$ . To describe a sample connected to contacts, absorbing boundary conditions ( $\partial_z K_{\delta B}(\mathbf{0}, \mathbf{r}) = 0$ ) should be imposed at  $z = 0$  and  $z = L$ . However, provided the size of a phase-coherent region is much smaller than the sample size, so that  $D\tau_{in} \ll L^2$ , it is sufficient to use the solution of Eq. (3.20) for a system of infinite extent in the  $z$ -direction when evaluating the right-hand side of Eq. (3.15). This solution is

$$K_{\delta B}(\mathbf{0}, \mathbf{r}) = (\hbar v)^{-2} \left( \frac{v}{4\pi D x} \right)^{1/2} \exp(-S) \quad (3.21)$$

where

$$S = \frac{vz^2}{4Dx} + \frac{x}{l_{in}} - \frac{i\delta\beta xz}{2} + \frac{D(\delta\beta)^2 x^3}{12v}. \quad (3.22)$$

Combining Eqns. (3.15), (3.18), and (3.21), we obtain

$$F(\delta B) = J_0^2 L C \int_0^\infty dx \int_{-\infty}^\infty dz |K_{\delta B}(\mathbf{0}, \mathbf{r})|^2 \quad (3.23)$$

and so find the correlation function for conductance fluctuations given in Eq.(2.3)

The form of the scaling function  $f(y)$  is shown in Fig. 2. It is normalised so that  $f(0) = 1$ , and decreases as

$f \propto y^{-1/6}$  for  $y \gg 1$ , so that the conductance correlation function decays as  $F(\delta B) \propto |\delta B|^{-1/3}$  for large  $|\delta B|$ .

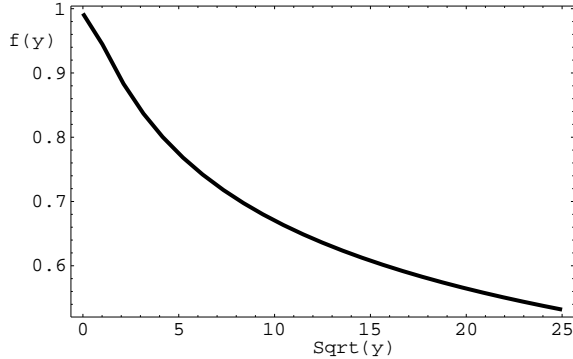


FIG. 2. The scaling function  $f(y)$

### 2. Weakly coupled edges: $\tau_{in}^{-1} \gg \tau_{\perp}^{-1}$

If adjacent edges are sufficiently weakly coupled by tunneling, there is mesoscopic regime in which the inelastic scattering rate is small, in the sense that  $\tau_{in}^{-1} \ll \tau_{el}^{-1}$ , but the interlayer tunneling rate is even smaller. It is sufficient in this regime to calculate the conductance correlation function at leading order in the interlayer coupling,  $t$ . Doing so, we retain  $t$  in the current operators but use Green's functions for a system of isolated edges. The disorder-averaged single-particle Green's function in this limit

is

$$G^R(E; \mathbf{r}_1, \mathbf{r}_2) = \Theta(x_2 - x_1) \delta_{n_1, n_2} \times (i\hbar v)^{-1} \exp(-[(2l_{in})^{-1} - i\beta an_1][x_2 - x_1]), \quad (3.24)$$

where  $\Theta(x)$  is the step function. The short-range terms associated with current operators in Eq. (3.15) may then be approximated as

$$J(\mathbf{r}, \mathbf{r}') = \frac{J_0}{2} \delta(x - x') [\delta_{n, n'+1} + \delta_{n, n'-1}]. \quad (3.25)$$

The diffusion propagator reduces for uncoupled edges to a function which has a phase determined by  $\delta B$  and which decays in amplitude with distance only as a result of inelastic scattering. We take it to be

$$K_{\delta B}(\mathbf{r}_1, \mathbf{r}_2) = \Theta(x_2 - x_1) \delta_{n_1, n_2} \times (\hbar v)^{-2} \exp(-[l_{in}^{-1} - i\delta \beta an_1][x_2 - x_1]). \quad (3.26)$$

Combining Eqns. (3.15), (3.25), and (3.26), we obtain

$$F(\delta B) = \frac{1}{4} J_0^2 N C \times \int_0^\infty dx [K_{\delta B}(0, n; x, n) K_{\delta B}^*(0, n+1; x, n+1) + \text{c.c.}] \quad (3.27)$$

and hence arrive at the correlation function for conductance fluctuations given in Eq.(2.8).

### D. Conductance fluctuations in energy

It is also of interest to consider the dependence of conductance fluctuations on Fermi energy. In particular, the range of conductance correlations in energy for a system at zero temperature will determine the extent to which the amplitude of fluctuations measured at finite temperature is reduced by thermal smearing of the electron distribution. We find that conductance fluctuations are perfectly correlated in energy. To show this, we return to Eq. (3.15) but replace the magnetic field difference  $\delta B$  with an energy difference  $\delta E$ . The diffusion propagator at finite energy difference simply acquires a phase:

$$K_{\delta E}(\mathbf{r}, \mathbf{r}') = K(\mathbf{r}, \mathbf{r}') e^{i\delta E(x' - x)/(\hbar v)}. \quad (3.28)$$

This phase cancels when  $K_{\delta E}(\mathbf{r}_1, \mathbf{r}_2)$  and  $K_{\delta E}^*(\mathbf{r}_4, \mathbf{r}_3)$  are combined, since the factors  $J(\mathbf{r}, \mathbf{r}')$  associated with the current operators are short-range, so that  $\mathbf{r}_1 \approx \mathbf{r}_4$  and  $\mathbf{r}_2 \approx \mathbf{r}_3$  in Eq. (3.15). As a consequence, the correlation of conductance fluctuations is independent of  $\delta E$ . The physical reason for this behaviour is that, if  $\psi_n(x)$  is an eigenfunction of Eq. (3.1) for some realisation of disorder, with energy  $E$ , then  $\psi'_n(x) \equiv e^{i\omega x/v} \psi_n(x)$  is also an eigenfunction, with energy  $E' = E + \hbar\omega$ , provided  $\omega C/v$  is an integer multiple of  $2\pi$ , so that periodic boundary conditions in the chiral direction are satisfied. Hence, apart from the phase factor, which does not affect the conductance, states are perfectly correlated in energy. As a result, the only consequence of a change in temperature is a change in the inelastic scattering rate.

## IV. EFFECTS OF INTERACTIONS

### A. Polarization and screening

In this section we study several aspects of electron-electron interactions in the chiral metal. As a first step, it is necessary to examine screening of the Coulomb interaction between a pair of electrons, by other electrons in the Fermi sea. One can expect the frequency and wavevector dependence of the screened interaction to be significant. In conventional conductors, the consequence of disorder and the resulting diffusive motion of charge (with diffusion constant  $D$ ) is that screening of a potential having wavevector  $q$  is suppressed<sup>22</sup> at frequencies higher than  $Dq^2$ . And in a one-dimensional chiral metal at the edge of a two-dimensional integer quantum Hall system, electron-electron interactions modify the dispersion relation for edge magneto-plasmons<sup>31</sup>. We find in

the two-dimensional chiral metal that dynamical screening at finite wavevector interpolates, as a function of the direction of the wavevector, between these two types of behaviour.

Our results may be obtained either by using the random phase approximation within a diagrammatic calculation, or more transparently from a hydrodynamic approach, as follows.

Consider the response of the chiral metal to a space- and time-dependent external potential. Let  $\rho(\mathbf{r}, t)$  be the screening charge density induced in the presence of an electric field that has components  $(E_x, E_z)$  within the surface. We require an equation of motion for  $\rho(\mathbf{r}, t)$ , which we derive in the usual way, by considering  $\mathbf{J}(\mathbf{r}, t)$ , the deviation from equilibrium of the current density, and using the continuity equation. Treating the transverse direction as continuous, one has

$$J_x(\mathbf{r}, t) = v\rho(\mathbf{r}, t) \quad (4.1)$$

and

$$J_z(\mathbf{r}, t) = -D\partial_z\rho(\mathbf{r}, t) + \sigma E_z, \quad (4.2)$$

so that the effect of the transverse component of the electric field is simply to generate a transverse current density. The effect of the component of the electric field in the chiral direction is rather different: referring to the three-dimensional sample as a whole,  $E_x$  generates Hall currents within each layer, which transport charge between the bulk and the surface. The resulting change in surface charge density may be represented by adding a term to the continuity equation, so that it becomes

$$\partial_t\rho(\mathbf{r}, t) = -\nabla \cdot \mathbf{J}(\mathbf{r}, t) + \frac{\sigma_H}{a}E_x, \quad (4.3)$$

where  $\sigma_H$  is the quantised Hall conductance of a layer, and (as in preceding sections)  $a$  is the layer spacing. It is helpful to express the conductivities in Eqns. (4.2) and (4.3) as  $\sigma = e^2nD$  and  $\sigma_H = e^2/h$ , and to recall that the density of states is  $n = (hva)^{-1}$ . Then, combining Eqns. (4.1), (4.2) and (4.3), the charge density evolves as

$$\begin{aligned} \partial_t\rho(\mathbf{r}, t) = & \\ -v\partial_x\rho(\mathbf{r}, t) + D\partial_z^2\rho(\mathbf{r}, t) + e^2n[vE_x - D\partial_zE_z]. \end{aligned} \quad (4.4)$$

The electric field appearing in these equations arises from a scalar potential  $\Phi_{tot}(\mathbf{r}, t)$  which is the sum of an externally imposed potential,  $\Phi_{ext}(\mathbf{r}, t)$ , and the potential  $\Phi_{scr}(\mathbf{r}, t)$  due to the screening charge,  $\rho(\mathbf{r}, t)$ . These last two quantities are related in the standard fashion<sup>32</sup> by the Poisson equation for a three-dimensional electrostatic problem, with coordinates  $\mathbf{r} = (x, z)$  and  $y$ , in which the charge density is  $\rho(\mathbf{r}, t)\delta(y)$  and  $\Phi_{scr}(\mathbf{r}, t)$  is found by evaluating the three-dimensional potential at  $y = 0$ . Taking Fourier transforms, defined according to

$$\rho(\omega, \mathbf{k}) \equiv \int d^2\mathbf{r} \int dt e^{i(\mathbf{k}\cdot\mathbf{r} + \omega t)} \rho(\mathbf{r}, t), \quad (4.5)$$

and similarly for other quantities, one finds

$$\Phi_{scr}(\omega, \mathbf{k}) = U_0(\mathbf{k})\rho(\omega, \mathbf{k})/e^2, \quad (4.6)$$

where

$$U_0(\mathbf{k}) = \frac{e^2}{2\epsilon_r\epsilon_0|\mathbf{k}|} \quad (4.7)$$

is the Fourier transform of the unscreened interaction potential between a pair of electrons. Expressing the electric field in terms of  $\Phi_{tot}(\mathbf{r}, t)$  and solving the Fourier transform of Eq. (4.4), we find

$$\Phi_{tot}(\omega, \mathbf{k}) = \frac{\Phi_{ext}(\omega, \mathbf{k})}{1 + U_0(\mathbf{k})\Pi(\omega, \mathbf{k})}, \quad (4.8)$$

where

$$\Pi(\omega, \mathbf{k}) = n \frac{Dk_z^2 - ivk_x}{Dk_z^2 - i\omega - ivk_x}. \quad (4.9)$$

This result simplifies in several limits. Static screening ( $\omega = 0$ ) is isotropic and as given by Thomas-Fermi theory, with an inverse screening length  $\kappa = e^2n/2\epsilon_r\epsilon_0$ . Dynamical screening of a potential with Fourier components only in the transverse direction ( $k_x = 0$ ) is exactly as in a non-chiral disordered, two-dimensional metal. Response to a potential with Fourier components only in the chiral direction ( $k_z = 0$ ) is undamped, and excitations have the dispersion relation:  $\omega = -v(k_x + \kappa)$ .

In the following, we shall treat interactions in the chiral metal using the Matsubara formalism. Within this approach, we find for the polarisation operator

$$\Pi(i\omega_n, \mathbf{k}) = n \frac{Dk_z^2 - ivk_x \text{sgn}(\omega_n)}{Dk_z^2 + |\omega_n| - ivk_x \text{sgn}(\omega_n)} \quad (4.10)$$

with  $\omega_n = 2\pi n k_B T$ , which has, as its analytical continuation, Eq. (4.9). Similarly, the screened Coulomb interaction potential is

$$U_{scr}(i\omega_n, \mathbf{k}) = U_0(\mathbf{k})/[1 + U_0(\mathbf{k})\Pi(i\omega_n, \mathbf{k})].$$

## B. Tunneling density of states

The enhanced interaction between slowly relaxing density fluctuations in a conventional, diffusive metal is responsible for a zero-bias anomaly in the tunneling density of states<sup>23</sup>. Balents and Fisher<sup>2</sup> have argued that such a zero-bias anomaly should not be expected in the chiral metal. Physically, charge that tunnels into the system is swept away at the chiral velocity; mathematically, the terms in perturbation theory associated with this anomaly yield only smooth contributions for the chiral metal.

In the present subsection we examine in more detail the reasons for this. It is sufficient for the purpose to consider a static interaction,  $U(\mathbf{r})$ , with finite range, between electrons separated by a distance  $\mathbf{r}$ , and to calculate at first order in  $U(\mathbf{r})$  the disorder-averaged exchange energy<sup>30</sup>. Let  $\Sigma(E)$  be the disorder-average of this quantity for an electron at energy  $E$  interacting with a filled Fermi sea<sup>22</sup>. The change in the density of states due to interactions is

$$\delta n(E) = -n \frac{d\Sigma(E)}{dE}. \quad (4.11)$$

Viewed in this way, the zero-bias anomaly in conventional, diffusive metals arises because states lying close in energy have wavefunctions which are highly correlated in space, enhancing interactions. Moreover, the wavefunction correlations depend strongly on the energy separation of the states, so that  $\Sigma(E)$  varies rapidly with  $E$  if  $E$  is close to the Fermi energy,  $E_F$ .

Let  $\{\Psi_\alpha(\mathbf{r})\}$  and  $\{E_\alpha\}$  be single-particle eigenfunctions and eigenenergies in a disordered chiral metal. The disorder-averaged exchange energy is

$$\Sigma(E) = -\frac{1}{n} \int_{-\infty}^{E_F - E} d\omega \int d^2\mathbf{r} U(\mathbf{r}) A(\omega, \mathbf{r}), \quad (4.12)$$

where the two-particle spectral function,  $A(\omega, \mathbf{r})$ , is defined by

$$A(\omega, \mathbf{r}) = \langle \sum_{\alpha\beta} \delta(E_\alpha) \delta(\omega - E_\beta) \Psi_\alpha^*(\mathbf{0}) \Psi_\alpha(\mathbf{r}) \Psi_\beta^*(\mathbf{r}) \Psi_\beta(\mathbf{0}) \rangle.$$

This spectral function can be calculated from the real part of the diffusion propagator, Eq. (3.4), or by considering the time-Fourier transform of the density associated with a spreading wavepacket. It has the form

$$A(\omega, \mathbf{r}) = \frac{1}{a(\hbar v)^2} \left( \frac{v}{4\pi D|x|} \right)^{1/2} \exp\left(-\frac{vz^2}{4D|x|} - \frac{i\omega x}{v}\right). \quad (4.13)$$

Combining Eqns. (4.11), (4.12) and (4.13), one sees that, if the potential has range  $R$ , then  $\delta n(E)$  is independent of  $E$  for  $|E - E_F| < \hbar v/R$ .

Inspecting Eq. (4.13), it is clear that eigenfunctions in the chiral metal do in fact have strong correlations:  $A(\omega, \mathbf{r})$  with  $\mathbf{r} = (x, z)$  diverges as  $|x| \rightarrow 0$  for  $z = 0$ . These correlations, however, depend only weakly on energy, and so do not produce a large change in the tunneling density of states.

## C. Inelastic scattering rate

The following subsection is devoted to a calculation of the contribution from electron-electron interactions to the inelastic scattering rate,  $\tau_{in}^{-1}$ , which acts as a cut-off for conductance fluctuations.

We compute  $\tau_{in}^{-1}$  by finding at leading order the interaction contribution to the irreducible vertex that appears in the ladder sum for the diffusion propagator used in calculations of conductance fluctuations<sup>27–29</sup>. The two single-particle (advanced and retarded) Green's functions from which this diffusion propagator is constructed are associated with distinct measurements of the conductance. In consequence, one should not include in the irreducible vertex diagrams in which the interaction line connects the two single-particle propagators. The relevant diagrams<sup>29</sup> are shown in Fig. 3, in which the full lines represent single-particle propagators, wavy lines are the screened Coulomb interaction, single dashed lines are impurity averages, and double dashed lines are diffusion ladders. We evaluate these diagrams treating the transverse direction as continuous, so that our results are restricted to the regime in which edges are strongly coupled:  $\tau_\perp^{-1} \gg \tau_{in}^{-1}$ . We set the energy and wavevector differences,  $\omega$  and  $\mathbf{q}$ , at the vertex to zero, express sums on Matsubara frequencies as contour integrals, and combine terms. We expect that the dominant contribution to the resulting integral will be from small wavevectors and energies, and use the asymptotic form of the integrand appropriate for this regime, obtaining

$$\begin{aligned} \tau_{in}^{-1} = & \frac{1}{\pi\hbar n} \int \frac{d^2\mathbf{q}}{(2\pi)^2} \int_{-\infty}^{+\infty} dx \times \\ & [\coth(x/2k_B T) - \tanh((x)/2k_B T)] \times \\ & \frac{x(\hbar D q_z)^2}{[(x + \hbar v q_x)^2 + (\hbar D q_z)^2][(\hbar v q_x)^2 + (\hbar D q_z)^2]}. \end{aligned} \quad (4.14)$$

The dependence of this expression on  $T$ ,  $D$  and  $v$  is made apparent by introducing the scaled variables:  $X = x/k_B T$ ,  $Q_x = \hbar v q_x/k_B T$  and  $Q_z = (\hbar D/k_B T)^{1/2} q_z$ . The integral can be evaluated numerically, yielding the expression for  $\tau_{in}$  given in Eq. (2.9). The physical interpretation of this result has been discussed in Sec. II.

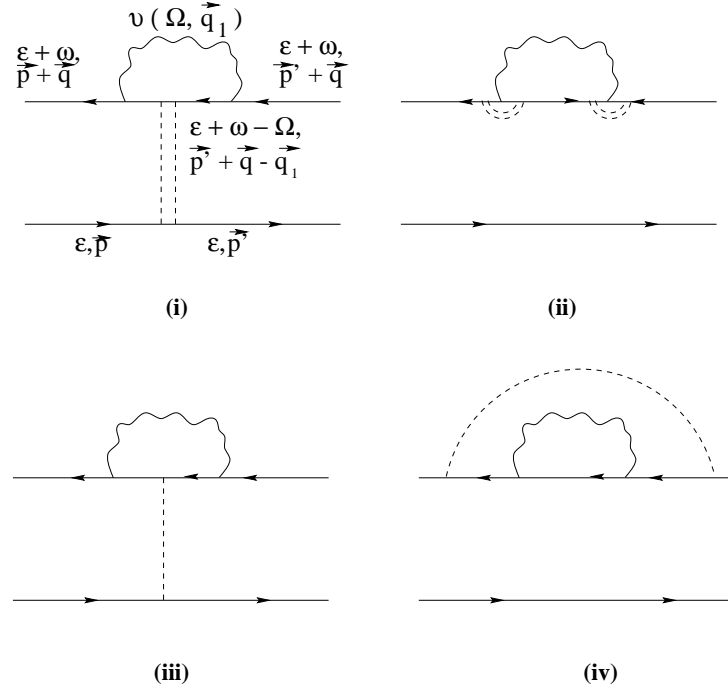


FIG. 3. The diagrams from which the inelastic scattering rate is calculated.

#### D. Interaction corrections to conductivity

Electron-electron interactions are known in diffusive conductors to give rise to temperature-dependent contributions to the conductivity that are singular in the low-temperature limit<sup>24–26</sup>. The origin of these interaction corrections to the conductivity is similar to that of the zero-bias anomaly in the tunneling density of states. Since the chiral metal has no zero-bias anomaly, one expects it to have no singular interaction contribution to the conductivity. In the following subsection we outline calculations that confirm this at leading order. The presentation follows closely that of Altshuler, Khmel'nitskii, Larkin, and Lee<sup>26</sup> for the diffusive metal.

To compute the interaction correction to the conductivity of the chiral metal using the Matsubara technique, it is convenient to use the Kubo formula in the form

$$\sigma = \lim_{\omega \rightarrow 0} \frac{i\Lambda(\omega)}{\omega} \quad (4.15)$$

where  $\Lambda(\omega)$  is the analytic continuation in  $\omega$  of

$$\Lambda(i\omega_n) = \frac{k_B T}{A} \sum_{\epsilon_m} \langle \text{Tr}[j_z g(i[\epsilon_m + \omega_n]) j_z g(i\epsilon_m)] \rangle. \quad (4.16)$$

The diagrams that contribute to  $\Lambda(i\omega_n)$  at leading order in the screened interaction strength can be classified according to the number of diffusion propagators each one contains. Those with the most diffusion propagators are most singular in the low-temperature limit. They can be separated into two categories. Diagrams in the first category are illustrated in Fig. 4, corresponding to Figs. 5(a), 5(b) and 5(c) of Ref. 26. It has been shown for a diffusive conductor in Ref. 26 that these cancel, and we find the same to be true in the chiral metal. Diagrams in the second category are illustrated in Fig. 5, corresponding to Figs. 5(d) and 5(e) of Ref. 26. For the two-dimensional diffusive metal, these diagrams make a contribution to the conductivity which is logarithmic in temperature. For the chiral metal, their contribution is formally proportional to  $T^{1/2}$ , but with a numerical coefficient which we find to be zero after integrating over the component in the chiral direction of the momentum transferred by the interaction.

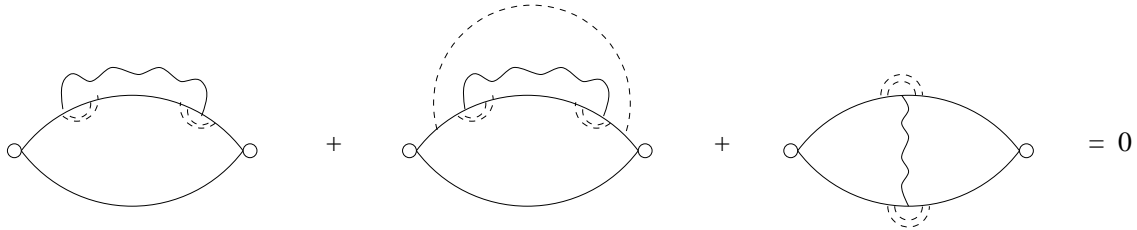


FIG. 4. Diagrams for the interaction correction to the conductivity which cancel.

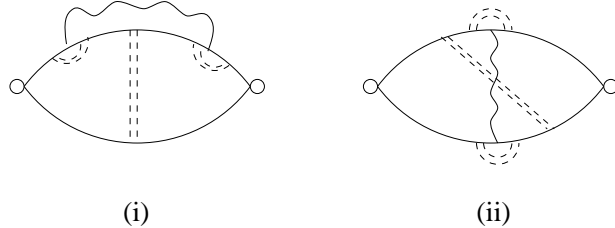


FIG. 5. The remaining leading-order diagrams for the interaction correction to the conductivity.

## V. DISCUSSION

Our results, as set out in Sec. II, are a contribution to the understanding of transport in the chiral metal. In many senses, it is a particularly simple example of a disordered conductor. Quantum interference effects are suppressed by chiral motion, and interaction effects are less singular than in diffusive two-dimensional conductors. We have provided a rather detailed treatment of conductance fluctuations, which we hope will be tested experimentally. We have also identified a distinct mesoscopic regime, for weakly coupled edges, in which the inter-edge tunneling rate,  $\tau_{\perp}^{-1}$ , is smaller than the inelastic scattering rate,  $\tau_{in}^{-1}$ . In this regime, transport is controlled by the properties of an isolated, one-dimensional chiral metal.

Recent experiments<sup>17,18</sup> appear, in fact, to probe behaviour of weakly coupled edges, though their analysis has necessarily so far been based on theory for the opposite regime. According to that analysis, the inelastic scattering length in the transverse direction, estimated from the variance of conductance fluctuations using Eq. (2.1), is shorter than the inter-layer spacing, even at the lowest temperatures investigated. Moreover, this estimate of the inelastic scattering length is inconsistent with the value deduced from the correlation field for conductance fluctuations, using Eq. (2.2), as one might expect if the theory used is, in fact, inappropriate. It will be interesting to find whether these discrepancies are resolved by using the theory we have presented to analyse the experiments. If so, such measurements provide a way to investigate interaction effects in a one-dimensional system of chiral fermions.

## ACKNOWLEDGMENTS

We are particularly grateful for discussions and correspondence with D. P. Druist and E. G. Gwinn. We also thank L. Balents, F. H. L. Essler, I. A. Gruzberg, R. A. Smith, and A. M. Tsvelik for useful discussions. J.B. acknowledges partial financial support from the European Union through the Marie Curie Grant; the work was also supported in part by EPSRC under Grant No GR/J8327.

## REFERENCES

- <sup>1</sup> J. T. Chalker and A. Dohmen, Phys. Rev. Lett. **75**, 4496 (1995).
- <sup>2</sup> L. Balents and M. P. A. Fisher, Phys. Rev. Lett. **76**, 2782 (1996).
- <sup>3</sup> D. P. Druist, P. J. Turley, K. D. Maranowski, E. G. Gwinn, and A. C. Gossard, Phys. Rev. Lett. **80**, 365 (1998).
- <sup>4</sup> H. L. Störmer, J. P. Eisenstein, A. C. Gossard, W. Wiegmann, and K. Baldwin, Phys. Rev. Lett. **56**, 85 (1985); H. L. Störmer *et al.* *Proceedings of the 18th International Conference on the Physics of Semiconductors, Stockholm, 1986*, edited by O. Engstrom (World Scientific, Singapore, 1987), p. 385.
- <sup>5</sup> Y. B. Kim, Phys. Rev. B **53**, 16 420 (1996).
- <sup>6</sup> H. Mathur, Phys. Rev. Lett. **78**, 2429 (1997).
- <sup>7</sup> Y.-K. Yu, cond-mat/9611137 (unpublished).
- <sup>8</sup> L. Balents, M. P. A. Fisher, and M. R. Zirnbauer, Nucl. Phys. B **483**, 601 (1997).

<sup>9</sup> I. A. Gruzberg, N. Read, and S. Sachdev, Phys. Rev. B **55**, 10 593 (1997).

<sup>10</sup> I. A. Gruzberg, N. Read, and S. Sachdev, Phys. Rev. B **56**, 13 218 (1997).

<sup>11</sup> S. Cho, L. Balents, and M. P. A. Fisher, Phys. Rev. B **56**, 15 814 (1997).

<sup>12</sup> Z. Q. Wang, Phys. Rev. Lett. **78** 126 (1997); *ibid* **79**, 4002 (1997).

<sup>13</sup> V. Plerou and Z. Q. Wang, Phys. Rev. B **58**, 1967 (1998).

<sup>14</sup> Y. Meir, Phys. Rev. B **58**, R1762 (1998).

<sup>15</sup> J. T. Chalker and S. L. Sondhi, Phys. Rev. B **59**, 4999 (1999).

<sup>16</sup> J. J. Betouras and J. T. Chalker, Proceedings of the Conference *Les Rencontres de Moriond* on “Quantum Physics at the Mesoscopic Scale” (1999).

<sup>17</sup> D. P. Druist, K. H. Yoo, P. J. Turley, E. G. Gwinn, K. Maranowski, and A. C. Gossard, Superlattices and Microstructures, **25**, 181 (1999).

<sup>18</sup> E. G. Gwinn, unpublished (1998), talk at the Conference on “Disorder and Interactions in Quantum Hall and Mesoscopic Systems”, ITP Santa Barbara (1998).

<sup>19</sup> B. Zhang, J. S. Brooks, Z. Wang, J. A. A. J. Perenboom, J. Simmons, J. Reno, N. Lumpkin, J. O’Brien, and R. Clark, Physica B **258**, 279 (1998).

<sup>20</sup> S. Hill, P. S. Sandu, J. S. Qualls, J. S. Brooks, M. Tokumoto, N. Kinoshita, T. Kinoshita, and Y. Tanaka, Phys. Rev. B **55**, R4891 (1997); M. M. Honold, N. Harrison, J. Singleton, H. Yaguchi, C. Mielke, D. Rickel, I. Dekkers, P. H. P. Reinders, F. Herlach, M. Kurmoo, and P. Day, J. Phys. Cond. Matt. **9**, L533 (1997); S. Uji, C. Terakura, M. Takashita, T. Terashima, H. Aoki, J. S. Brooks, S. Tanaka, S. Maki, J. Yamada, and S. Nakatsuji, Phys. Rev. **60**, 1650, (1999).

<sup>21</sup> S. Hill, S. Uji, M. Takashita, C. Terakura, T. Terashima, H. Aoki, and J. S. Brooks, Phys. Rev. B **58**, 10778 (1998).

<sup>22</sup> For reviews, see: B. L. Altshuler and A. G. Aronov, in *Electron - electron Interactions in Disordered Systems*, edited by A. L. Efros and M. Pollak (North- Holland, Amsterdam, 1985), p. 1; and I. L. Aleiner, B. L. Altshuler, and M. E. Gershenson, Waves in Random Media, **9**, 201 (1999), and references therein.

<sup>23</sup> B. L. Altshuler and A. G. Aronov, Zh. Eksp. Teor. Fiz. **77**, 2028 (1979) [Sov. Phys. JETP **50**, 968 (1979)].

<sup>24</sup> B. L. Altshuler and A. G. Aronov, Solid State Commun. **36**, 115 (1979).

<sup>25</sup> B. L. Altshuler, A. G. Aronov, and P. A. Lee, Phys. Rev. Lett. **44**, 1288 (1980).

<sup>26</sup> B. L. Altshuler, D. Khmel’nitzkii, A. I. Larkin, and P. A. Lee Phys. Rev. B **22**, 5142 (1980).

<sup>27</sup> B. L. Altshuler and A. G. Aronov, Zh. Eksp. Teor. Fiz. Pis’ma Red. **30** 514 (1979) [JETP Lett **30**, 482 (1979)].

<sup>28</sup> E. Abrahams, P. W. Anderson, P. A. Lee and T. V. Ramakrishnan, Phys. Rev. B **24**, 6783 (1981).

<sup>29</sup> For a recent discussion, see: Ya. M. Blanter, Phys. Rev. B **54**, 12807 (1996).

<sup>30</sup> There is no Hartree correction to the density of states in the chiral metal because impurity scattering does not generate density fluctuations.

<sup>31</sup> V. A. Volkov and S. A. Mikhailov Sov. Phys. JETP **67**, 1639 (1988).

<sup>32</sup> T. Ando, A. B. Fowler and F. Stern, Rev. Mod. Phys. **54**, 437 (1982).